



Photoinitiated polymerization of PEG-diacrylate with lithium phenyl-2,4,6-trimethylbenzoylphosphinate: polymerization rate and cytocompatibility

Benjamin D. Fairbanks^a, Michael P. Schwartz^a, Christopher N. Bowman^a, Kristi S. Anseth^{a,b,*}

^aDepartment of Chemical and Biological Engineering, University of Colorado, Boulder, Colorado 80309-0424, USA

^bHoward Hughes Medical, Institute, University of Colorado, Boulder, Colorado 80309-0424, USA

ARTICLE INFO

Article history:

Received 8 August 2009

Accepted 26 August 2009

Available online 23 September 2009

Keywords:

Photopolymerization

Hydrogel

Cytotoxicity

Poly(ethylene oxide)

Fibroblast

ABSTRACT

Due to mild reaction conditions and temporal and spatial control over material formation, photopolymerization has become a valuable technique for the encapsulation of living cells in three dimensional, hydrated, biomimetic materials. For such applications, 2-hydroxy-1-[4-(2-hydroxyethoxy)phenyl]-2-methyl-1-propanone (I2959) is the most commonly used photoinitiator (by virtue of its moderate water solubility), yet this initiator has an absorption spectrum that is poorly matched with wavelengths of light generally regarded as benign to living cells, limiting the rate at which it may initiate polymerization in their presence. In contrast, acylphosphine oxide photoinitiators, generally exhibit absorption spectra at wavelengths suitable for cell encapsulation, yet commercially available initiators of this class have low water solubility. Here, a water soluble lithium acylphosphinate salt is evaluated for its ability to polymerize diacrylated poly(ethylene glycol) (PEGDA) monomers rapidly into hydrogels, while maintaining high viability during direct encapsulation of cells. Through rheometric measurements, the time to reach gelation of a PEGDA solution with the phosphinate initiator is one tenth the time for that using I2959 at similar concentrations, when exposed to 365 nm light. Further, polymerization with the phosphinate initiator at 405 nm visible light exposure is achieved with low initiator concentrations and light intensities, precluded in polymerizations initiated with I2959 by its absorbance profile. When examined 24 h after encapsulation, survival rates of human neonatal fibroblasts encapsulated in hydrogels polymerized with the phosphinate initiator exceed 95%, demonstrating the cytocompatibility of this initiating system.

© 2009 Elsevier Ltd. All rights reserved.

1. Introduction

Photoinitiated polymerization is an attractive technique for the *in situ* formation of hydrogels as it provides unparalleled spatial and temporal control over the formation of the material. Photopolymerizations are also generally advantageous as a means for cellular encapsulation, based on their rapid reaction rates which enable facile encapsulation without significant cell settling, and the ability to initiate the polymerization without a need for high temperatures or extreme pH conditions in a non-purged environment [1]. Additionally, in contrast to spontaneously polymerizing hydrogels (e.g., Michael addition, enzymatically crosslinked, self-assembled), premature gelation is not an obstacle to the user's application of the material as the polymerization is controlled temporally and initiated on demand. In general, photopolymerization

for the encapsulation of living cells has proven a useful tool for the study of cellular behavior in three dimensions, as well as for various biomedical applications [2–6].

Radical photopolymerizations are initiated by the combination of irradiation with appropriate wavelengths of light and the presence of a distinct species that absorbs that light. The absorbing species then decomposes, or facilitates the decomposition of a coinitiator species, into radicals that initiate polymerization. Radical photoinitiating systems are broadly divided into two classes associated with their radical generation mechanism following photon absorption. Type I (cleavage type) photoinitiators dissociate into two radicals following photon absorption, while type II initiating systems, in an excited state after photon absorption, abstract a hydrogen atom from a second, coinitiator species [7]. Of the type II photoinitiating systems, camphorquinone–amine combinations have been applied with some success in cellular photoencapsulations [8], and Hubbell et al. have succeeded in employing eosin Y (a fluorescent cellular cytoplasm stain) as a cytocompatible photoinitiator [9,10]. Eosin is highly water soluble and initiates polymerization when exposed

* Corresponding author. Howard Hughes Medical, Institute, University of Colorado, Boulder, Colorado 80309-0424, USA.

E-mail address: kristi.anseth@colorado.edu (K.S. Anseth).

to green light. However, eosin Y suffers from several practical drawbacks. Being a type II photoinitiator, it requires a coinitiator and often accelerant species to generate efficiently a sufficient number of radicals for photopolymerization [9,10]. Furthermore, the excitation and emission spectra of eosin Y overlap with many fluorophores commonly used in cellular imaging which complicates subsequent use of such dyes.

Most commercial type I initiators, particularly those with visible light absorbance, have limited water solubility and high cell toxicity [8]. Currently, the UV initiator (Fig. 1) 1-[4-(2-hydroxyethoxy)-phenyl]-2-hydroxy-2-methyl-1-propanone (Irgacure 2959 or I2959 from Ciba Specialty Chemicals, Tarrytown, NY) is the most commonly used photoinitiator for cellular encapsulation within hydrogels [8,11,12], despite significant limitations. Although it is among the most water-soluble of the commercially available type I photoinitiators, its solubility limit in water at ambient conditions is reportedly less than 2 wt% [13]; however, even 0.5 wt% solutions require substantial agitation and/or heating to dissolve the initiator completely. While limited water solubility is a drawback to the use of I2959, the initiator possesses a greater intrinsic shortcoming. For efficient polymerization an initiator should have an absorbance spectrum that exhibits good overlap with the emission spectrum of the desired light source; however, for cellular encapsulation lower wavelength light is precluded because of its phototoxic and mutagenic characteristics [14–16]. Often, emission from the light source is filtered to allow light centered at 365 nm. The molar extinction coefficient of I2959 at 365 nm, however, is very low ($4 \text{ M}^{-1} \text{ cm}^{-1}$) and trails off almost entirely before 370 nm [8], limiting the photoinitiated polymerization kinetics at or near these wavelengths. Polymerization at longer wavelengths, such as visible or violet light initiated polymerization, is precluded by effectively zero absorption of the light by I2959.

Majima et al. [17] demonstrated the synthesis of a lithium acylphosphinate salt (Fig. 1) as a water-soluble (up to 8.5 wt%) photoinitiator for polymerization of several unsaturated monomers in water-containing solutions for micelle and graft copolymerization applications. Here, this photoinitiator is demonstrated to be a cytocompatible, type I photoinitiator that permits the encapsulation of human neonatal fibroblasts in poly(ethylene glycol) diacrylate (PEGDA) hydrogels. The application of this acylphosphinate salt results in improved polymerization kinetics, enabling cell encapsulations at lower initiator concentrations and longer wavelength light relative to I2959. The synthesis, purification and subsequent chemical characterization are presented in detail. Further, photobleaching and attenuation of light in thick hydrogel samples are specifically addressed.

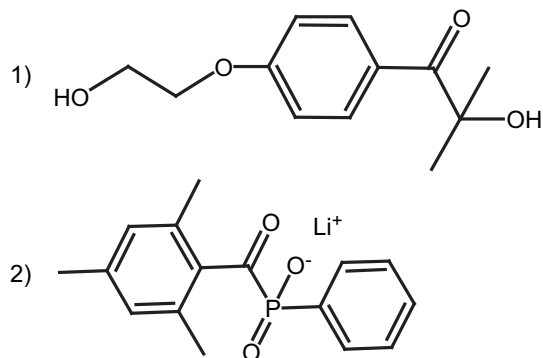


Fig. 1. Chemical structures of the photoinitiator 1-[4-(2-hydroxyethoxy)-phenyl]-2-hydroxy-2-methyl-1-propanone (I2959) (1) and lithium phenyl-2,4,6-trimethylbenzoylphosphinate(LAP) (2).

2. Methods

2.1. Initiator synthesis

The initiator was synthesized in a two step process as originally described by Majima et al. [17]. Dimethyl phenylphosphonite (Acros Organics) was reacted with 2,4,6-trimethylbenzoyl chloride (Sigma–Aldrich) via a Michaelis–Arbuzov reaction. At room temperature and under argon, 3.2 g (0.018 mol) of 2,4,6-trimethylbenzoyl chloride was added dropwise to an equimolar amount of continuously stirred dimethyl phenylphosphonite (3.0 g). The reaction mixture was stirred for 18 h whereupon a four fold excess of lithium bromide (6.1 g) in 100 mL of 2-butanone (both from Sigma–Aldrich) was added to the reaction mixture from the previous step which was then heated to 50 °C. After 10 min, a solid precipitate formed. The mixture was cooled to ambient temperature, allowed to rest for four hours and then filtered. The filtrate was washed and filtered 3 times with 2-butanone to remove unreacted lithium bromide, and excess solvent was removed by vacuum. The product, lithium phenyl-2,4,6-trimethylbenzoylphosphinate, hereafter designated LAP for lithium acylphosphinate after the convention of similarly structured photoinitiators, BAPO and MAPO [18], was recovered in near quantitative yields.

2.2. Chemical characterization of initiator

Following synthesis of the initiator, several techniques were used to verify the structure and purity of the initiator. The initiator product was initially analyzed in D₂O via ¹H, ¹³C and ³¹P NMR. For the ¹H NMR spectrum, all peaks showed appropriate shifts and integrated quantitatively. For ¹³C and ³¹P NMR spectra, all peaks showed appropriate shifts. Carbon and phosphorus NMR characterization was performed on a Varian Inova–400 MHz NMR Spectrometer, while proton NMR was performed on a Varian Inova–500 MHz NMR Spectrometer (spectra available in Supporting information, Figs. S1–S6). Peaks consistent with the proposed structure were observed as follows: ¹H NMR (500 MHz, D₂O, δ): 7.57 (m, 2H), 7.42 (m, 1H), 7.33 (m, 2H), 6.74 (s, 2H), 2.09 (s, 3H), 1.88 (s, 6H); ¹³C NMR (400 MHz, D₂O, δ): 228.77 (d, J = 111 Hz), 140.11, 137.88 (d, J = 39 Hz), 133.88, 132.82 (d, J = 128 Hz), 132.38 (d, J = 9.5 Hz), 132.23 (d, J = 2.7 Hz), 128.56 (d, J = 12.3 Hz), 128.26, 20.27, 18.65; ³¹P NMR (400 MHz, D₂O, δ) 13.58. Electrospray ionization mass spec showed the expected m/z value of M⁻ = 287.0 amu (mass of salt compound minus the mass of lithium), corresponding to the mass of the proposed compound. In total, these techniques verified that the synthetic approach yielded the desired LAP initiator structure.

UV/Vis extinction coefficients for I2959 and LAP were determined from the absorbances of 4 mM initiator solutions in water as measured with a Perkin Elmer Lambda 40 UV–vis spectrometer. Photobleached products of the initiators were generated by the exposure of 4 mM solutions to 10 mW/cm² 365 nm light. Absorption spectra were taken periodically until absorbances stabilized, indicative of complete photolysis.

2.3. PEG diacrylate synthesis

The synthesis of the photopolymerizable poly(ethylene glycol)diacrylate (PEGDA) was performed under anhydrous conditions as described previously [19]. Briefly, acryloyl chloride (Sigma–Aldrich) in dry toluene was added dropwise to a constantly agitated solution of 1 molar equivalent triethylamine and 0.8 m equivalents of hydroxyls on 4600 Da PEG (Sigma–Aldrich) in dry toluene. PEGDA was retrieved from solution by precipitation in 4 °C diethyl ether.

2.4. Gelation

In situ dynamic photorheology [20] was used to measure the elastic and viscous moduli during photopolymerization. An Ares 4400 rheometer from TA Instruments was modified to enable simultaneous moduli measurements and irradiation of the sample. A mirror, 45° to the upper plate, directed light down through a hollow shaft and through the quartz plate to the sample, allowing dynamic, real-time monitoring of evolving moduli during light exposure (see Supplementary Fig. S7 for equipment setup). For determining the storage (G′) and loss (G″) moduli crossover point, representing a time near the critical gel point conversion [21], dynamic time sweep measurements were taken during sample exposure with a frequency of 10 Hz and a strain of 10% gap width for each sample. Plate separation was 120 μm and the plate diameter was 20 mm. Linearity at 10% strain was verified prior to and following polymerization with a strain sweep from 1% to 100% gap width.

2.5. Cell encapsulation and viability

For cell encapsulation studies, human neonatal foreskin fibroblasts were encapsulated in phosphate buffered saline solution with 10 wt% 4600 Da molecular weight PEGDA and indicated initiator concentration at a seeding density of 1×10^6 cells/mL. The gels were polymerized between glass microscope slides separated by rubber gaskets with circular holes punched out, forming disc-shaped molds for the hydrogel/cell constructs. The total volume of each gel was approximately 40 mL with a diameter of 7 mm and a thickness of 1 mm. Following polymerization, hydrogel discs were removed and placed in DMEM

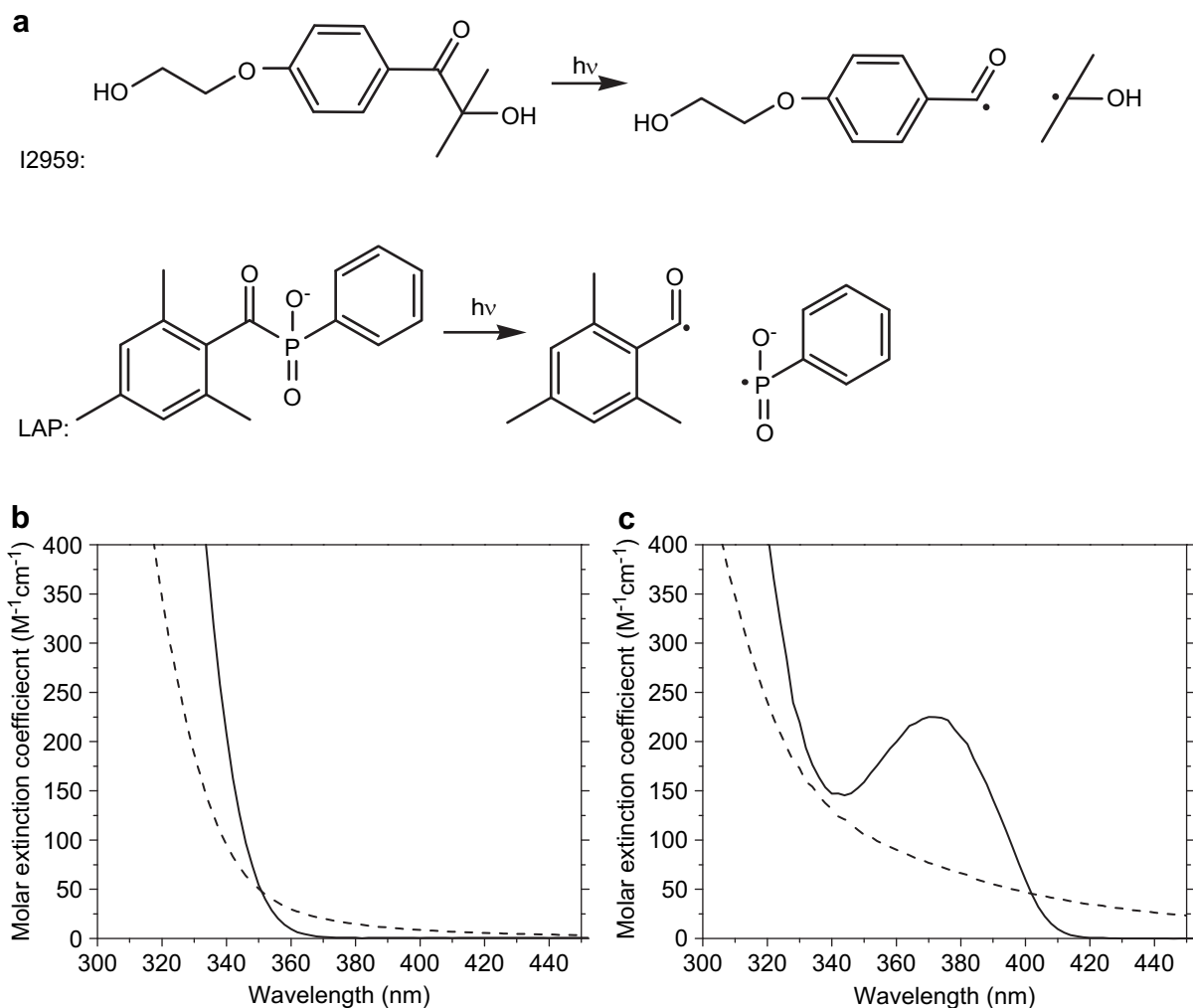


Fig. 2. (a) Cleavage of I2959 and LAP into substituent radicals following photon absorption. (b) Molar absorptivities of the I2959 (solid line) and cleavage products (dashed line). (c) Molar absorptivities of LAP (solid line) and cleavage products (dashed line).

medium (Invitrogen) supplemented with 10% fetal bovine serum (Invitrogen). The cell-laden gel materials were incubated under standard conditions, 37 °C and 5% CO₂, for 24 h, whereupon cell viability was determined using the Live/Dead[®] cytotoxicity kit (Invitrogen), a membrane integrity assay. Gels were incubated for 30 min in PBS with 2 μm calcein, which stains live cells green and 4 μm ethidium homodimer, which stains the nuclei of dead cells red. Encapsulated cells were imaged on a Zeiss 510 confocal microscope, three gels per condition, three images taken at random coordinates within each gel for a total of nine images per condition. Live cells were counted using MetaMorph software while dead cells were counted manually.

2.6. Polymerization light source

Ultraviolet initiating light for both *in situ* dynamic rheometry and cell encapsulations was provided by a 100 W Hg short-arc lamp (Omnicure 1000, EXFO, Mississauga, Ont., Canada) with the manufacturer-supplied filter for 365 nm exposure (365 ± 5 nm at half max with a shoulder of 10% max transmission extending to 335 nm). Exposure at 405 nm was provided by an EXFO Acticure with the manufacturer-supplied 400–500 nm filter. The spectral output was further restricted by a 405 nm interference filter (405 ± 5 nm at half max) from Melles Griot (Irvine, CA). Spectral output data was provided by Exfo and Melles Griot for their respective filters.

3. Results and discussion

3.1. Absorption spectra for LAP and I2959

For chain polymerizations that exhibit classical non-chain length dependent bimolecular termination, the polymerization

rate is generally proportional to the square root of the initiation rate, R_i [22]. For photoinitiated polymerizations R_i is given by [7]

$$R_i = \frac{2\phi\epsilon f I C_i}{N_A h \nu} \quad (1)$$

Here, I is the incident light intensity (units of power/area, e.g. mW/cm²) and C_i is the initiator concentration. Intrinsic properties of the photoinitiator that influence its utility are ϵ , the molar extinction coefficient (absorbivity); ϕ , the quantum yield or cleavage events that occur per photon absorbed; and f , the photoinitiator efficiency or the ratio of initiation events to radicals generated by photolysis. Avogadro's number, N_A ; Plank's constant, h and the frequency of the initiating light, ν are included for unit conversion. This equation, presented here to demonstrate how the various parameters affect the utility and performance of an initiator, assumes a uniform light intensity (i.e., optically thin film) and monochromatic (i.e., single wavelength) exposure. Often, to improve the polymerization rate, I and C_i are increased, but higher light intensity and higher initiator concentrations can have cytotoxic effects [8,14]. Further, the low solubility of I2959 in water limits the maximum value of C_i in this system, and many light sources do not permit uniform, high intensity exposure over a large area. As seen in Fig. 2, LAP has a local absorbance maximum at

approximately 375 nm and significant absorbance at 365 nm (molar extinction coefficient at 365, $\epsilon = 218 \text{ M}^{-1} \text{ cm}^{-1}$). Additionally, the initiator measurably absorbs, albeit weakly, in the visible region from 400 nm to 420 nm. The absorbance of I2959 at 365 nm is very weak ($\epsilon = 4 \text{ M}^{-1} \text{ cm}^{-1}$) and does not rise above noise at wavelengths longer than 370 nm. As the initiation rate is directly proportional to the light absorbed by the photoinitiator as described by equation (1), the weak absorbance profile of I2959 severely limits its utility for photopolymerizations performed at 365 nm or longer wavelengths.

Also notable is the change in absorption by LAP following photocleavage. As the acylphosphinate is cleaved, the chromophore is lost. This loss is significant for the polymerizations of films that are not optically thin. For example, as the initiator towards the exposed surface is consumed, the light penetrates more deeply into the film and enhances the maximum cure depths that are achieved. This behavior is explored in more detail in a subsequent section (Section 3.3). In contrast, I2959 does not exhibit these advantageous bleaching characteristics as can be seen in Fig. 2b.

3.2. Time to gelation

As demonstrated in Fig. 3a, the time required to reach the gel point during the solution polymerization of PEGDA is approximately one order of magnitude lower for LAP than for I2959 with 365 nm illumination at comparable intensities and initiator concentrations. An example of the rheometric data used to determine gel point is presented in Supplementary Figs. S8 and S9. Presumably, a large part of this increased polymerization rate is due to the fact that LAP absorbs more light at this wavelength than does I2959 leading to a higher initiation rate. To normalize for the light absorbed by the photoinitiator, the gel point is plotted as a function of photons or light absorbed by the photoinitiator as described in equation (2) [23].

$$L = C_i \int_{\lambda_1}^{\lambda_2} \epsilon(\lambda) \cdot E(\lambda) d\lambda \quad (2)$$

The light absorbed per volume is represented by L ; E is the spectral output of the curing lamp as a function of wavelength (λ); and λ_1 and λ_2 are wavelengths outside of which the product $\epsilon(\lambda) \cdot E(\lambda) = 0$.

Even when normalized for the light absorption differences that exist between LAP and I2959, the LAP-initiated polymerization gels at earlier times (Fig. 3b). This outcome indicates that the initiation rate increase is due not only to the higher molar absorptivity of LAP, but also due to a higher quantum yield or a higher initiation efficiency, parameters ϕ and f respectively in equation (1). This conclusion is further supported when comparing the gel point data (crossover time) for photopolymerization of gels with LAP and either 365 nm or 405 nm light. In this case, the time to gelation collapses to a single curve when plotted as a function of light absorbed as would be expected for a given initiator molecule. Of further note, after an 1800 s exposure to 405 nm light, no gelation is observed in those samples prepared with I2959.

3.3. Attenuation

Because I2959 has only minimal absorption at 365 nm, light attenuation in thicker samples can generally be disregarded (optical densities of these films at 365 nm are all less than 0.001 cm^{-1}), but the higher absorbance of LAP that contributes to the more rapid polymerization necessitates that light attenuation be considered. The light intensity (I) at a particular depth in an optically thick sample is well described by equation (3) [24].

$$I(z, t) = I_0 e^{-2.303[\epsilon_i C_i(z, t) + \epsilon_b C_b(z, t)]z} \quad (3)$$

Here, z and t are the sample depth and exposure time, respectively; I_0 is the sample's incident light intensity; C_i and C_b are the concentration of the unreacted photoinitiator and the reacted, photobleached initiator fragments, respectively; and ϵ_i and ϵ_b represent the molar absorptivities of the photoinitiator and photobleached fragments. Ignoring diffusion of initiator and bleached initiator degradation products on the polymerization time scale, their respective concentration profiles are described by the following [24]:

$$\frac{\partial C_i(z, t)}{\partial t} = -\epsilon_i \phi \left(\frac{I(z, t)}{N_A h \nu} \right) C_i(z, t) \quad (4)$$

$$\frac{\partial C_b(z, t)}{\partial t} = \frac{\partial C_i(z, t)}{\partial t} \quad (5)$$

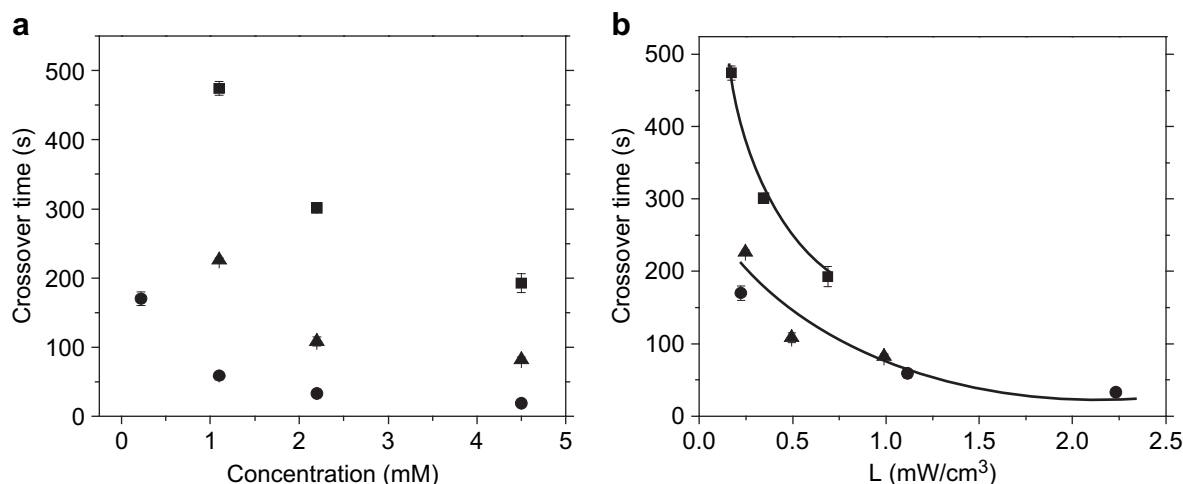


Fig. 3. Comparison of the solution polymerization of PEG-diacrylate initiated by either I2959 or LAP. Storage/loss moduli crossover, as a measure of the time required to achieve gelation, is plotted against the initiator concentration (a) and light absorbed by initiator (b). Squares represent samples prepared with I2959 and circles represent samples prepared with LAP polymerized at 5 mW/cm^2 365 nm filtered light at ambient temperature. Triangles represent samples polymerized with LAP at 10 mW/cm^2 405 nm filtered light. Solid lines provided for clarity only.

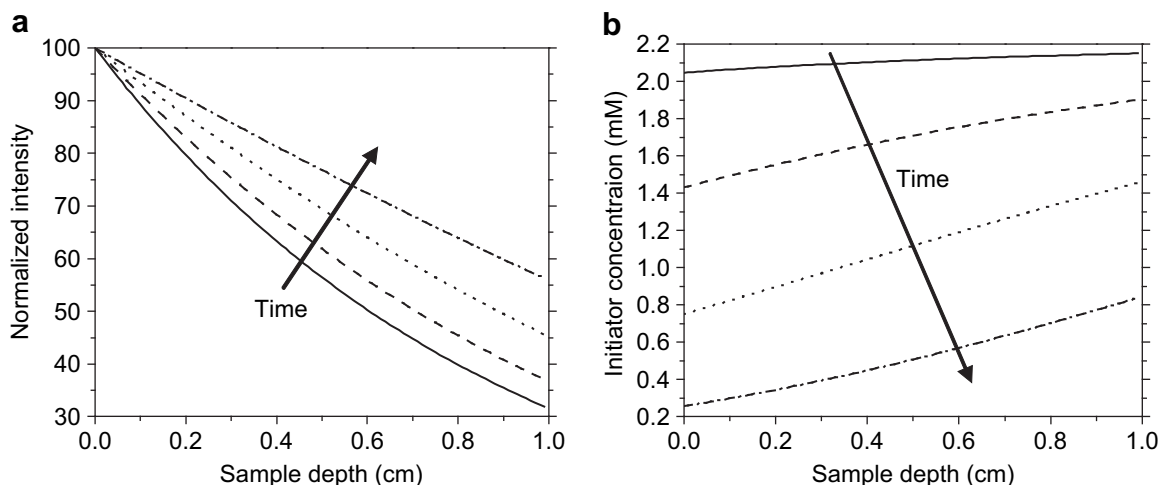


Fig. 4. Normalized light intensity, I/I_0 (a) and Initiator concentration (b) as a function of sample depth for 10 s (solid black line) 60 s (dashed line) 150 s (dotted line) and 300 s (dash-dot) of exposure to 365 nm light. Plots are generated with a presumption of an initial initiator concentration of 2.2 mM, a light intensity of 10 mW/cm² and assuming a quantum yield of 1.

According to equation (3) for an initial initiator concentration (C_i) of 2.2 mM (equivalent to 0.05 wt% I2959 or 0.067 wt% LAP), only 10% of the light is absorbed as it passes through a 1 mm thick sample (a common dimension for cell encapsulation experiments). In other words, the light intensity at the bottom of the gel is within approximately 10% of that at the top. Thus, it is expected that there are only minimal, relatively insignificant spatial gradients induced by the light attenuation in samples used here. Moreover, the bleaching characteristics of LAP, typical of acylphosphine oxide initiators [25] would further mitigate attenuation effects as the polymerization proceeds and initiator is consumed. Upon cleavage, as shown in Fig. 2a, the acylphosphinate chromophore is lost [26], and the absorbance below 400 nm drops substantially.

For those cases in which thicker samples must be cured, equations (3)–(5) may be solved simultaneously (assuming a quantum yield of unity) allowing the observation of trends of both light attenuation and initiator concentration with respect to time and depth (Fig. 4). Since a quantum yield of unity is assumed, these plots represent the minimum time over which such concentration gradients would be generated. The initiator concentration (C_i) and light exposure intensity (I_0) represented in Fig. 4 (2.2 mM and 10 mW/cm², respectively) were chosen as typical, reasonable conditions for cell encapsulation. Initially, 30% of the light penetrates a 1 cm sample, but as the initiator is consumed, more light (55% by five minutes) is permitted through. While attenuation is substantial under these conditions, even following initiator bleaching, decreasing initiator concentration and/or lengthening exposure time would certainly enable 1 cm and thicker gels to be cured.

3.4. Cytocompatibility

A variety of compounds have been explored previously as potentially cytocompatible photoinitiators [8,11]. Most of these initiators, particularly the cleavage type, such as 1-hydroxycyclohexyl phenyl ketone (Irgacure 184), 2,2-dimethoxy-2-phenylacetophenone (Irgacure 651), and 2-methyl-1-[4-(methylthio)phenyl]-2-(4-morpholinyl)-1-propanone (Irgacure 907) ultimately can be highly cytotoxic [8,11]. However, despite the toxicity of many related compounds, I2959 has been reported to exhibit relatively low cytotoxicity and has become a commonly used cleavage type photoinitiator for cell encapsulations and biomaterials applications [8,11,12]. Here, the relative cytotoxicity of LAP is evaluated by

determining the survival of cells encapsulated in PEGDA gels polymerized with LAP and compared to that of cells encapsulated in identical gels polymerized with I2959.

Because radicals themselves are highly reactive and often cytotoxic [8,27], a relevant experiment is the comparison of survival rates in polymerizations initiated with comparable number of radicals generated. Since the quantum yield under these reaction conditions is unknown, the polymerizations were carried out with initiator concentrations and illumination times to yield similar photon absorption. As seen in Table 1, cell survival in gels polymerized with 1 min exposure to 10 mW/cm² of 365 nm light exposure and 2.2 mM LAP was statistically similar to a 6 min polymerization with the same molar initiator concentration of I2959 (corresponding to 0.05 wt%) at the same light intensity. Likewise, a concentration of 0.22 mM LAP combined with 10 min of light exposure results in comparably high cell survival. Thus, significantly lower concentrations of photoinitiators are cytocompatible while still maintaining reasonable polymerization rates. This reduction is highly desirable to minimize leachables from the material after polymerization.

As previously discussed, I2959 is incapable of initiating polymerization under mild visible light illumination on a timescale of interest to those wishing to encapsulate cells, but photoencapsulation of cells with 10 mW/cm² exposure at 405 nm with 2.2 mM LAP is achieved in 5 min and results in ~96% cell viability. The ability to polymerize at longer wavelengths has significant benefits. Many dental lamps, endoscopic probes, microscope imaging lamps and lasers emit light in the short wavelength visible spectrum, but not at 365 nm or lower. Light emitting diodes (LEDs) are an increasingly popular light source for photopolymerizations due to their low energy requirements and uniform emission

Table 1

Cell survival at 24 h when photoencapsulated in PEG-diacrylate gels at various initiation conditions.

Initiator and concentration (mM)	Wavelength (nm)	Exposure time (min)	Energy absorbed by initiator (J/cm ³)	Gel time (s)	Survival (%)
2.2 mM I2959	365 nm	6	0.245	212	95 ± 3
2.2 mM LAP	365 nm	1	0.224	20	96 ± 2
0.22 mM LAP	365 nm	10	0.224	141	95 ± 2
2.2 mM LAP	405 nm	5	0.244	120	96 ± 2

spectra. Battery operated LED flashlights with 385 nm and 405 nm wavelength emissions are commonly available from a variety of vendors. These sources facilitate a more cost-effective, versatile and portable initiating light source than is currently customary.

4. Conclusion

The initiator, lithium phenyl-2,4,6-trimethylbenzoylphosphinate or LAP, was synthesized and characterized for its effectiveness in initiating polymerizations. Specifically, its potential for application to photoencapsulation of living cells was explored. The initiator demonstrated remarkable advantages over I2959, including greater water solubility, increased polymerization rates with 365 nm wavelength light, and absorbance above 400 nm that enables efficient visible light polymerization. Cell survival for fibroblasts encapsulated in LAP-initiated PEG diacrylate hydrogels was 95% or greater for every condition evaluated.

Acknowledgments

The authors thank Professor R. Rivkahlsseroff for supplying neonatal dermal fibroblasts. This work was supported by the National Institute of Health grant DE012998.

Appendix. Supplementary data

Supplementary data associated with this article can be found in the online version, at doi:10.1016/j.biomaterials.2009.08.055.

References

- [1] Bowman CN, Kloxin CJ. Toward an enhanced understanding and implementation of photopolymerization reactions. *AIChE J* 2008;54(11):2775–95.
- [2] Elisseeff J, Anseth K, Sims D, McIntosh W, Randolph M, Yaremchuk M, et al. Transdermal photopolymerization of poly(ethylene oxide)-based injectable hydrogels for tissue-engineered cartilage. *Plast Reconstr Surg* 1999;104(4):1014–22.
- [3] Burdick JA, Anseth KS. Photoencapsulation of osteoblasts in injectable RGD-modified PEG hydrogels for bone tissue engineering. *Biomaterials* 2002;23(22):4315–23.
- [4] Dumanian GA, Dascombe W, Hong C, Labadie K, Garrett K, Sawhney AS, et al. A new photopolymerizable blood-vessel glue that seals human vessel anastomoses without augmenting thrombogenicity. *Plast Reconstr Surg* 1995;95(5):901–7.
- [5] Mellott MB, Searcy K, Pishko MV. Release of protein from highly cross-linked hydrogels of poly(ethylene glycol) diacrylate fabricated by UV polymerization. *Biomaterials* 2001;22(9):929–41.
- [6] Quick DJ, Macdonald KK, Anseth KS. Delivering DNA from photocrosslinked, surface eroding polyanhydrides. *J Control Release* 2004;97(2):333–43.
- [7] Fouassier J-P. Photoinitiation, photopolymerization, and photocuring: fundamentals and applications. Munich: Carl Hanser Verlag; 1995.
- [8] Bryant SJ, Nuttelman CR, Anseth KS. Cytocompatibility of UV and visible light photoinitiating systems on cultured NIH/3T3 fibroblasts in vitro. *J Biomater Sci Polym Ed* 2000;11(5):439–57.
- [9] Cruise GM, Hegre OD, Scharp DS, Hubbell JA. A sensitivity study of the key parameters in the interfacial photopolymerization of poly(ethylene glycol) diacrylate upon porcine islets. *Biotechnol Bioeng* 1998;57(6):655–65.
- [10] Sawhney AS, Pathak CP, Hubbell JA. Interfacial photopolymerization of poly(ethylene glycol)-based hydrogels upon alginate poly(L-Lysine) microcapsules for enhanced biocompatibility. *Biomaterials* 1993;14(13):1008–16.
- [11] Williams CG, Malik AN, Kim TK, Manson PN, Elisseeff JH. Variable cytocompatibility of six cell lines with photoinitiators used for polymerizing hydrogels and cell encapsulation. *Biomaterials* 2005;26(11):1211–8.
- [12] Fedorovich NE, Oudshoorn MH, van Geemen D, Hennink WE, Alblas J, Dhert WJA. The effect of photopolymerization on stem cells embedded in hydrogels. *Biomaterials* 2009;30(3):344–53.
- [13] Fouassier JP, Burr D, Wieder F. Water-soluble photoinitiators - primary processes in hydroxy alkyl phenyl ketones. *J Polym Sci Part A Polym Chem* 1991;29(9):1319–27.
- [14] Kappes UP, Luo D, Potter M, Schulmeister K, Runger TM. Short- and long-wave UV light (UVB and UVA) induce similar mutations in human skin cells. *J Invest Dermatol* 2006;126(3):667–75.
- [15] Jones CA, Huberman E, Cunningham ML, Peak MJ. Mutagenesis and cytotoxicity in human epithelial-cells by far-ultraviolet and near-ultraviolet radiations - action spectra. *Radiat Res* 1987;110(2):244–54.
- [16] Kielbassa C, Roza L, Epe B. Wavelength dependence of oxidative DNA damage induced by UV and visible light. *Carcinogenesis* 1997;18(4):811–6.
- [17] Majima T, Schnabel W, Weber W. Phenyl-2,4,6-trimethylbenzoylphosphinates as water-soluble photoinitiators - generation and reactivity of O = P(C6H5)(O-) radical-anions. *Macromol Chem Phys* 1991;192(10):2307–15.
- [18] Decker C, Zahouily K, Decker D, Nguyen T, Viet T. Performance analysis of acylphosphine oxides in photoinitiated polymerization. *Polymer* 2001;42(18):7551–60.
- [19] Cruise GM, Scharp DS, Hubbell JA. Characterization of permeability and network structure of interfacially photopolymerized poly(ethylene glycol) diacrylate hydrogels. *Biomaterials* 1998;19(14):1287–94.
- [20] Chiou BS, English RJ, Khan SA. Rheology and photo-cross-linking of thiol-ene polymers. *Macromolecules* 1996;29(16):5368–74.
- [21] Winter HH. Can the gel point of a cross-linking polymer be detected by the G' - G' crossover. *Polym Eng Sci* 1987;27(22):1698–702.
- [22] Odian G, editor. Principles of polymerization. New York: Wiley; 1991.
- [23] Stahl F, Ashworth SH, Jandt KD, Mills RW. Light-emitting diode (LED) polymerisation of dental composites: flexural properties and polymerisation potential. *Biomaterials* 2000;21(13):1379–85.
- [24] Miller GA, Gou L, Narayanan V, Scranton AB. Modeling of photobleaching for the photoinitiation of thick polymerization systems. *J Polym Sci Part A Polym Chem* 2002;40(6):793–808.
- [25] Rutsch W, Dietliker K, Leppard D, Kohler M, Misev L, Kolczak U, et al. Recent developments in photoinitiators. *Prog Org Coat* 1996;27:227–39.
- [26] Dietliker K, Jung T, Benkhoff J, Kura H, Matsumoto A, Oka H, et al. New developments in photoinitiators. *Macromol Symp* 2004;217(1):77–98.
- [27] Kehrer JP. Free-radicals as mediators of tissue-injury and disease. *Crit Rev Toxicol* 1993;23(1):21–48.